Prabashni Lekha*, Tamara Bush, Norman Pammenter, Bruce Sitholè and Patricia Berjak

Quantitative assessment of xylan distribution across the secondary cell wall layers of *Eucalyptus* dissolving pulp fibres

https://doi.org/10.1515/hf-2017-0070
Received May 10, 2017; accepted August 15, 2017; previously published online September 13, 2017

Abstract: A quantitative method has been developed for assessment of the distribution of xylan across the secondary cell wall layers of *Eucalyptus* dissolving pulp fibres by means of a carbohydrate binding module (CBM), *Ct*CBM6, in combination with transmission electron microscopy (TEM). To ensure reproducibility and to minimise non-specific labelling, various parameters were optimised, namely the size of the gold colloid marker, *Ct*CBM6 concentration, and the selection of buffer solutions. The method was replicated on processed *Eucalyptus* fibres containing different xylan contents. Reproducible xylan counts and distributions across the secondary cell wall layers were obtained for unbleached and bleached *Eucalyptus* fibres. The xylan distribution pattern across the cell wall layers S1, S2 and S3 was similar, but the S1 and S3 layers contained after bleaching more xylan than the S2 layer. The technique has a wide range of applications in basic wood research as well as in the analysis of technological processes.

Keywords: carbohydrate binding module (CBM), eucalyptus, TEM, xylan

***Corresponding author: Prabashni Lekha,** Council for Scientific and Industrial Research (CSIR), Biorefinery Industry Development Facility, 359 Masizi Kunene Avenue, Durban 4013, South Africa, Phone: +2731 242 2331/+2731 261 1216, e-mail: plekha@csir.co.za
Tamara Bush: School of Chemistry, University of KwaZulu-Natal (UKZN), Durban 4001, South Africa
Norman Pammenter and Patricia Berjak: School of Life Sciences, UKZN, Durban 4001, South Africa
Bruce Sitholè: Council for Scientific and Industrial Research (CSIR), Biorefinery Industry Development Facility, 359 Masizi Kunene Avenue, Durban 4013, South Africa; and Discipline of Chemical Engineering, UKZN, Durban 4001, South Africa

Introduction

During dissolving pulp production, hemicelluloses and lignin are removed from the fibre wall resulting in a high purity α-cellulose pulp. The residual hemicelluloses within the fibre wall after bleaching affect the performance (reactivity) and quality (brightness) of dissolving pulp (Wilson and Tabke 1974; Sixta 2006; Wollboldt et al. 2010). Xylan is the main hemicellulose component of hardwood fibre cell walls (Timell 1967) and the knowledge about the quantity and distribution of xylan within hardwood fibre walls is helpful to understand the parameters responsible for variations in performance and quality of dissolving pulps.

The spatial distribution of the cell wall polysaccharides is also relevant in basic scientific questions and in the context of other technological processes, which were for a long time a domain of immunoassay detection methods. For example: Altaner et al. (2007) detected the β-1-4-galactan in compression wood of Sitka spruce by immunofluorescence; Fernando and Daniel (2008) observed the glucomannan distribution in the cell wall of Scots pine in the context of thermomechanical processing (TMP) processing; Gao et al. (2014) and Kim et al. (2015) detected the distribution of hemicelluloses and pectins in the cell wall by immunocytochemistry in a softwood and a hardwood during the Termovuoto (heat treatment) process; Blumentritt et al. (2016) observed the changes of glucomannans and xylans in the poplar cell wall in the course of hot water treatment. However, in the focus of the present study is the technique based on carbohydrate binding modules (CBMs), which is simpler than the time consuming immunolabelling.

CBMs have been identified as useful tools for localisation of complex carbohydrate molecules (McCartney et al. 2006; Shoseyov et al. 2006; Filonova et al. 2007a; Oliveira et al. 2015). CBMs are natural non-catalytic substrate-binding domains of several enzymes, which are associated with carbohydrate metabolism (Boraston et al. 1999). The primary action of CBMs increases the catalytic efficiency of the carbohydrate-active enzymes for soluble and/or insoluble substrates (Hashimoto 2006). CBMs have been

divided into 53 families and classified into the groups A, B and C based on amino acid sequences and structural similarities (see Carbohydrate Binding Module Family Server http://afmb.cnrs-mrs.fr/~pedro/CAZY/cbm.html).

Particular CBMs attach to their target ligands with high specificity and affinity and are therefore valuable tools as molecular probes (Hashimoto 2006; Shoseyov et al. 2006; Pattathil et al. 2015). These are alternatives to antibody probes because they are smaller (e.g. typically <20 kDa vs. ~150 kDa for antibodies) and show specificity for individual carbohydrates (Ding et al. 2006; Filonova et al. 2007b; Oliveira et al. 2015; Pattathil et al. 2015). Furthermore, the ease of their production and modification with peptides and fluorescent and gold markers for microscopy is also encouraging (Filonova et al. 2007b).

Cellulose in wood fibre cell walls has been localised by CBMs (Mclean et al. 2002; Hildén et al. 2003; Daniel et al. 2006; Ding et al. 2006; Filonova et al. 2007a), such as xylan (McCartney et al. 2006; Filonova et al. 2007b), and mannan (Filonova et al. 2007a). McCartney et al. (2006) studied the affinity of six different xylan-specific CBMs in binding to primary and secondary cell walls for several dicotyledonous species. That study showed that CBMs from the families 2b, 4, 6, 15, 22 and 35 have a large range of specificities for natural ligands in the plant cell walls. It was concluded that the variation of CBM specificity for ligands may also be useful for the detection of distinct xylans in the cell wall (McCartney et al. 2006). Synthetically engineered xylan-binding CBMs were applied to target xylan molecules in birch and pine wood sections and birch kraft pulp fibres, and Filonova et al. (2007b) demonstrated that these kind of CBMs conjugated to fluorescein isothiocyanate (FITC) exhibit higher binding signals in delignified tissues compared to mature (normal) birch and pine wood. The CBMs in the quoted study were conjugated to the fluorescent dye [fluorescein isothiocyanate (FITC)], and the specimens were viewed by fluorescence microscopy. That method affords a lower resolution than transmission electron microscopy (TEM) and scanning electron-microscopy (SEM), therefore, the information on spatial distribution of hemicellulose molecules across the different cell wall layers was limited.

The family 6 CBM was the focus of the present study, which was isolated from *Clostridium thermocellum* xylanase 11A (Czjzek et al. 2001). The quoted authors determined the crystal structure of this module, which was resolved at 2.1 Å. The protein was characterised as a β-sandwich, which contains two potential ligand-binding clefts named as clefts A and B. By the combined application of nuclear magnetic resonance (NMR) spectroscopy coupled with site-directed mutagenesis, cleft A was identified as the ligand binding site. The CBM contains a surface loop that prevents cleft B from binding to the ligand. This module was established as being primarily a xylan binding CBM having the ability to bind to both decorated and undecorated xylan molecules (Verma et al. 2015).

Biological probes for localisation of carbohydrates within a matrix are necessarily a customised process for each tissue type as well as for the molecule being targeted (Horisberger 1979). Each protocol has to be refined to obtain a maximum specificity. The aim of the present study was to develop a reproducible method to map the distribution of xylan in *Eucalyptus* dissolving pulp fibres, which were unbleached and fully bleached. The intention was to understand better the xylan extraction process during bleaching, which is relevant for the production of high purity cellulose products. Bleached and unbleached materials were selected because of the clear differences in their xylan contents.

Materials and methods

Materials: Unbleached and fully bleached dissolving pulp fibres of *Eucalyptus* GU clone (*Eucalyptus grandis* W. Hill ex Maiden and *Eucalyptus urophylla* S.T. Blake) were investigated. The pulps were produced in the laboratory by acid bisulfite pulping and four subsequent bleaching steps as described by Chunilall et al. (2010).

Preparation of samples for TEM: The wood and pulp fibres were dehydrated in a serial dilution of ethanol (25, 50, 75 and 100%) and thereafter infiltrated slowly with London Resin (LR) white for 3 days. The samples were polymerised for 22 h at 60°C in gelatin capsules. All chemicals and reagents were purchased from Merck (Pty) Ltd, Modderfontein, South Africa unless otherwise stated.

Carbohydrate binding module (CBM): The *Ct*CBM6 (Prozomix, UK), a family 6 xylan-binding module, was used, which was isolated from *Clostridium thermocellum*. It was supplied as a 1 ml 3.2 M ammonium sulfate [$(NH_4)_2SO_4$] suspension, which contained 0.3 mg ml^{-1} CBM.

Preparation of a CBM stock solution: To maximise the activity of the CBM, solutions of 20 mM Tris-HCl, pH 7.5, 20 mM NaCl, 5 mM $CaCl_2$, and 0.05% (w/v) BSA were tested as stock solutions. The 1 ml 3.2 M $(NH_4)_2SO_4$ CBM suspension was divided into two aliquots, placed in Eppendorf tubes (1.5 ml), and centrifuged for 2 min at 13 225 *g*; the supernatant was then removed from each preparation and the resultant pellet was diluted with either 20 mM Tris-HCl buffer or 0.05% BSA.

Conjugation of gold colloid to the CBM: Three gold colloid nanoparticles with different size were tested for conjugation to the CBM, i.e. 20 nm (Sigma-Aldrich), 10 nm and 5 nm, which were prepared in the laboratory according to Dykstra and Reuss (2003) and Slot and Geuze (1981, 1985), respectively. In summary, the following solutions were prepared: (a) 1 ml 1% aqueous chloroauric acid with 100 ml DDW,

which was then reduced with 2.2 ml of 1% aqueous sodium citrate at 100°C (20 nm); (b) 80 ml DDW to which 1 ml 1% chloroauric acid was added; and (c) 4 ml 1% sodium citrate to which 16 ml DDW and 80 µl 1% tannic acid were added (10 nm gold particles) or (d) 4 ml 1% sodium citrate to which 16 ml DDW and 1 ml 1% tannic acid were added (5 nm gold particles). Solutions (b) and (c) or (b) and (d) were heated to 60°C, mixed and then heated to boiling on a hot plate to produce 10 nm and 5 nm gold particles, respectively. Combinations of the mixtures turned burgundy red after 2 min, which is an indicator for the production of nano-size particles. Investigation of the mixture on a JEOL 1010 TEM instrument revealed that 20 nm, 10 nm and 5 nm gold colloid particles had been formed, respectively. The gold colloid particles were coated with a 1% aqueous solution of polyethylene glycol (PEG) 20,000 (Sigma-Aldrich) prior to adjusting the pH, as gold particles are known to clog the electrode pores (Stannard 1998). In addition, PEG stabilises the gold colloid and prevents possible formation of aggregates (Horisberger and Vauthey 1984). The gold colloid solutions were adjusted to a pH at the theoretical isoelectric point of the CBM (one decimal point exact), which was calculated by the program ProtParam (theoretical isoelectric point calculator). For *Ct*CBM6, the calculated isoelectric point is 5.50.

Preparation of the CBM-gold colloid complex: The optimised concentration of CBM (i.e. 0.01 µg µl^{-1}) was placed in a 1.5 ml Eppendorf tube followed by adding 500 µl of gold colloid solution and 50 µl of 1% PEG. This solution was incubated at 4°C for 5 min and then centrifuged at the same temperature for 150 min at 15 338 *g*. After centrifugation, the supernatant was removed and the red sediment was dispersed in 75 µl 0.05% PEG and 300 µl of Tris-HCl buffer (pH 7.5).

Labelling with *Ct*CBM6-gold colloid complex: Table 1 describes the sequential steps required during labelling of ultra-thin sections using the *Ct*CBM6-gold colloid complex.

Control experiments: Two different control treatments were run in parallel to the experiments to ensure the specificity of the CBM reactions. The first control involved the application of gold colloid only for labelling ultra-thin sections. The second control involved a treatment of ultra-thin sections with the CBM solution (at the same concentration as applied for the complex preparation) for 30 min, with the attempt to saturate all the available binding sites. Thereafter, the same ultra-thin sections were incubated with the CBM-gold colloid complex.

Table 1: The sequential steps involved in localising xylan in unbleached and bleached dissolving pulp fibres, using CBM-gold labelling.

Step no.	Chemical	Duration (min)
1	0.05 M phosphate buffer saline (PBS, pH 7.0) + 50 mM glycine	15
2	PBS, pH 7.0	5
3	Blocking solution (PBS, containing 10% [v/v] foetal bovine serum, 1% bovine serum albumin [w/v], 0.05% [v/v] Tween-20 and 02% [w/v] sodium azide)	30
4	DDW	5
5	CBM-gold complex	30
6	DDW	5
7	PBS, pH 7.0, three sequential applications	10 each
8	DDW three sequential rinses	10 each

Method validation: Data sets from the CBM-gold methods were compared with xylan amounts obtained by high performance liquid chromatography (HPLC) (TAPPI test methods T249 cm-85, 1996–1997), which is supposed to be reliable as it is mostly applied in industrial laboratories for analysis of various liquid samples. To achieve a consistent mass of cellulose in the sample, the required pulp mass was 0.2 g (oven-dry, containing 90% cellulose and 60% moisture). The sample was then placed in a conical flask and hydrolysed with 3 ml of 72% sulfuric acid in a water bath for 1 h at 30°C ± 3°C. Thereafter the samples were rinsed with deionised water, placed in 250 ml screw-capped bottles (Schott, USA) and autoclaved for 1 h at 120°C–130°C (0.12–0.14 MPa pressure). The hydrolysate was then cooled to room temperature and filtered through 0.45 µm nylon filters (Membrane Solutions®, Separations, SA). The filtrate was then diluted 1:25 with de-ionised water and analysed for its monosaccharide content by HPLC-pulsed amperometric detector (PAD) (Rocklin and Pohl 1983; Hausalo 1995).

Staining, image capture, replication and analysis of images: The grids were subsequently stained with saturated aqueous uranyl acetate (2 min) to provide the necessary contrast in the specimens for TEM observations (JEOL TEM-1010, 100 kV). Image-Pro® Analyser 7.0 (SMM Instruments, SA) was applied. For each experiment, five images were collected per fibre and a total of 10 fibres were analysed, i.e. 50 micrographs were analysed. The gold particles in the different secondary cell wall layers were counted by a specially designed macro. Results are presented as a distribution of gold particles per µm^{-2} in images captured at the same magnification across the wall layers S1, S2 and S3.

The error bars in the graphs are for the mean ± standard error (SE): SE = mean SD/√sample number. Statistical analyses were performed by SPSS 19.0 for Windows. The level of significance for all statistical analyses performed was taken to be $P < 0.05$.

Results and discussion

*Ct*CBM6-gold colloid conjugates

The size of the gold colloid particle proved to be crucial affecting conjugation between the CBM and gold colloidal particles. A red sediment, which indicates a positive result after conjugation, was obtained only in case of 5 nm gold colloid particles (Table 2). Additionally, the CBMs were supplied in a 3.2 M $(NH_4)_2SO_4$ solution, and no conjugation occurred, if the CBM was not initially precipitated from the solution by centrifuging the required aliquot for 2 min and removing the $(NH_4)_2SO_4$ supernatant. The resultant red sediment was then diluted in the same volume of DDW prior to adding the gold colloid solution. The best centrifugation time was 150 min for the 5 nm gold particles as indicated by the clear supernatant after centrifugation, in

Table 2: Experiments performed with *Ct*CBM6 using different size gold colloid particles at pH 5.60.

*Ct*CBM6 Conc. (μg μl^{-1})	Gold colloid Size (nm)	Gold colloid Vol. (μl)	Centr. time (min)	Results	Colour of supernatant
0.08	20	500	70	–	Clear (black sediment of unconjugated gold at bottom of Eppendorf tube)
0.08	20	1000	70	–	
0.15	20	500	70	–	
0.08	10	500	80	–	
0.08	10	1000	120	–	
0.15	10	500	120	–	
0.30	10	500	120	–	
0.08	5	500	80	+	Pink
0.08	5	1000	120	+	Light pink
0.08	5	500	150	+	Clear

(–) no sediment; (+) red sediment (CBM-gold conjugation).

contrast to 80 and 120 min centrifugation times, which left a light pink coloured supernatant (Table 2).

Preparation of *Ct*CBM6 stock solution

The preparation of a CBM stock solution was necessary for optimisation. A 20 mM tris-HCl and 0.05% BSA solutions were tested for the preparation of the stock solution. The unbleached and fully bleached pulp fibre samples showed similar average total CBM-gold counts and the same distribution patterns, irrespective of the solvent applied (Figure 1a). However, a high level of background labelling was obtained in case of 0.05% BSA application, which was absent in the 20 mM tris-HCl stock solution.

Different *Ct*CBM6 concentrations for unbleached fibres

Four different CBM concentrations were tested *viz*, 0.01, 0.03, 0.05, 0.08 μg μl^{-1}. Concentrations above 0.01 μg μl^{-1} produced non-specific label on the resin, and all treatments resulted in the same distribution pattern across the secondary cell wall of unbleached fibres (Figure 1b). Thus a *Ct*CBM6 concentration of 0.01 μg μl^{-1} was selected as the best concentration to ensure specific labelling in further experimental steps.

Control experiments to ensure specificity *Ct*CBM6

A first control experiment was performed with gold colloid only without conjugation to the CBM and a negligible binding was found (Figure 2a). This result confirmed that the labelling is not due to the gold colloid in the CBM-gold

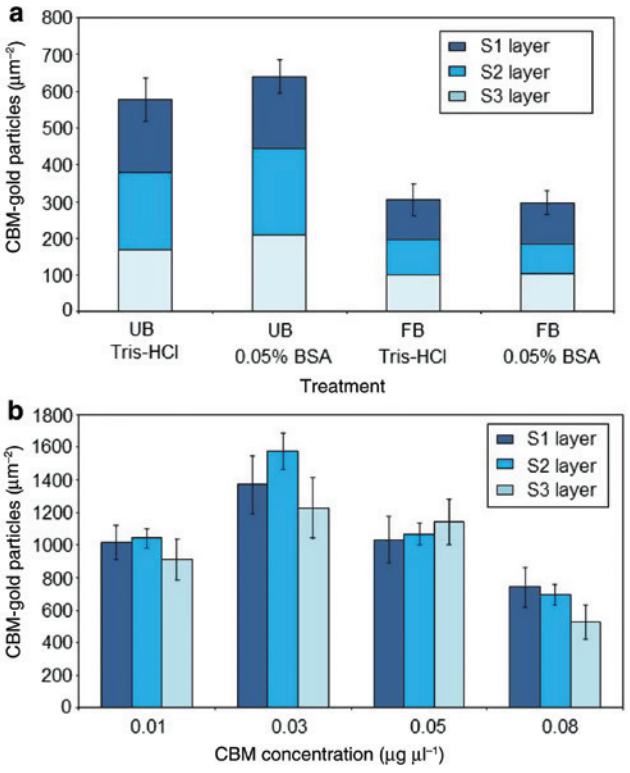

Figure 1: Optimisation of the CBM-gold labelling procedure to establish optimal buffer and CBM concencentration.
(a) CBM-gold counts obtained when using 20 mM Tris-HCl, pH 7.5 and 0.05% BSA for the preparation of the CtCBM6 stock solution. (UB, unbleached; FB, fully bleached). Error bars indicate standard error; $n = 10$; (b) Labelling of unbleached pulp fibres using different concentrations of the *Ct*CBM6 stock preparation in 20 mM Tris-HCl. Error bars indicate standard error; $n = 10$.

complex, but the CBM itself binds to xylan. The second control experiment was performed to ensure that the CBM is not heterogeneous (Polak and Van Noorden 1987). The available binding sites on the ultra-thin section were saturated with unconjugated CBM, and thereafter the same

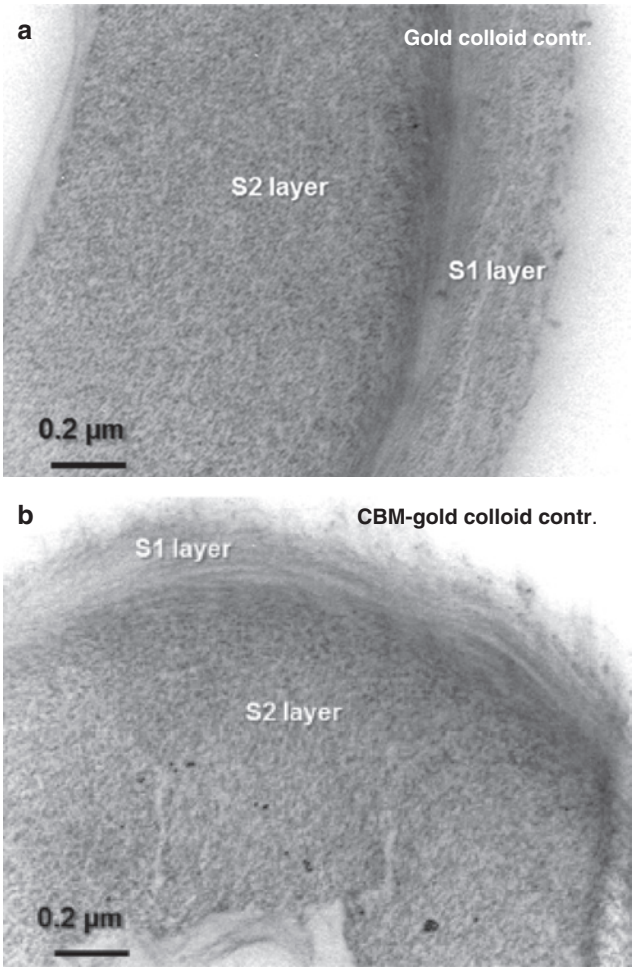

Figure 2: Control experiments were performed to assess reliability of the CBM-gold probe using unbleached fibres (a) gold colloid control; (b) CBM-gold colloid control.

sections were exposed to a CBM-gold conjugate. Also this control showed negligible binding to the section surface (Figure 2b), further illustrating that the same ligand is being targetted irrespective of the conjugation of CBM to the gold colloid. The bond between gold colloid and macromolecules has been shown to be non-covalent without an apparent change in the specific bio-activity of the latter (Horisberger 1979; Goodman et al. 1981).

Validation of the *Ct*CBM6-gold method

The total CBM-gold counts for xylan obtained for unbleached (bleaching step 1 and 2) and fully bleached pulp fibres are compared with xylan data obtained for the same samples by HPLC-PAD analysis (Figure 3). The CBM-gold and HPLC methods are very different techniques, nevertheless, the trends observed were similar with respect to the expected decline in xylan during

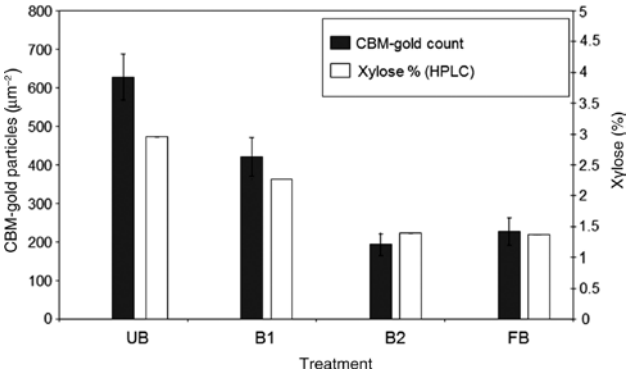

Figure 3: Comparison of CBM-gold counts with HPLC data for *Eucalyptus* unbleached and in-process bleached fibres.

bleaching, showing that the CBM-gold method responds to the removal of xylan from the pulp fibres. HPLC-PAD is a reliable technique, but it does not provide any data about the spatial distribution of xylan. Thus the CBM-gold approach is a valuable supplement to HPLC-PAD from the bleaching perspective. Figure 4 shows the CBM-gold

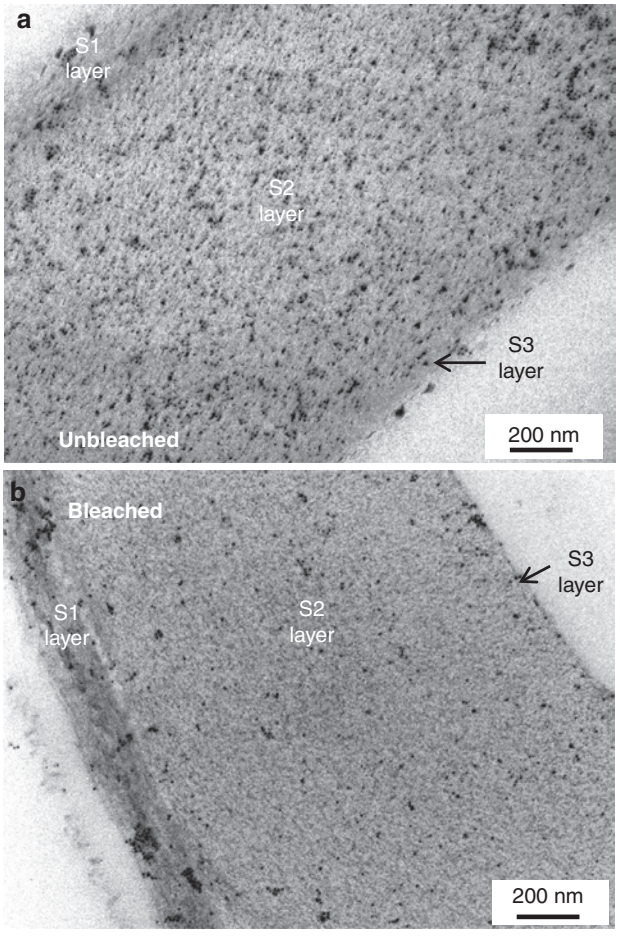

Figure 4: The optimal CBM-gold complex preparation used to label (a) unbleached and, (b) fully bleached, fibre cross-sections.

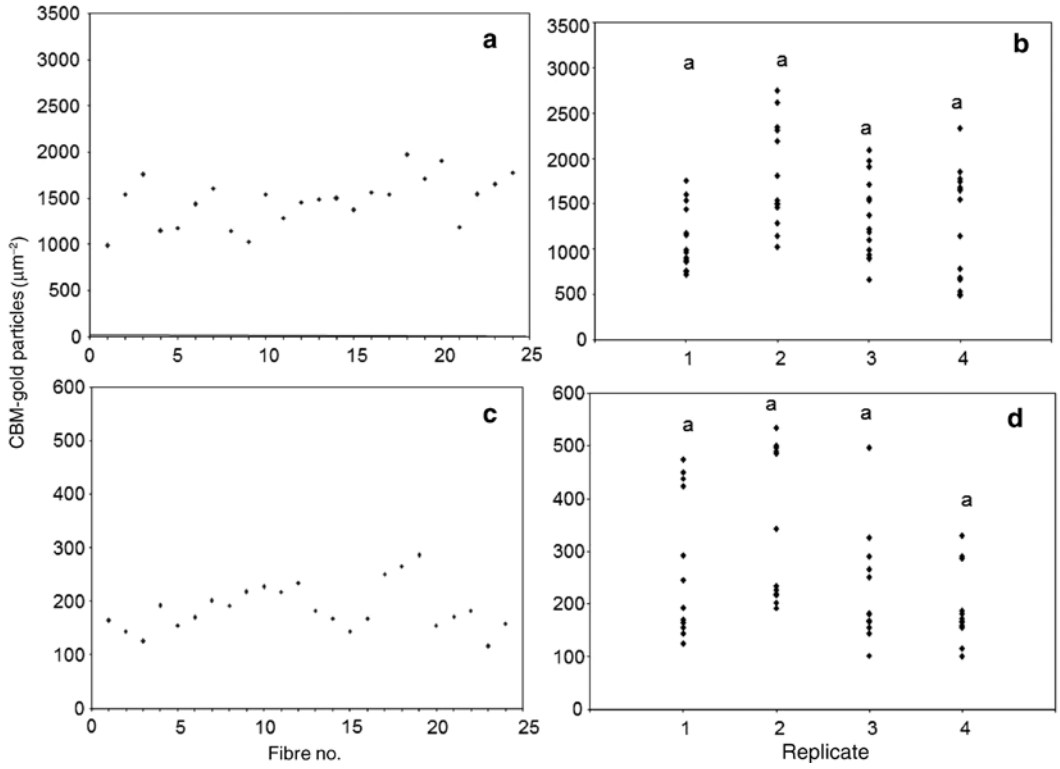

Figure 5: Reproducibility of xylan counts shown for replicate experiments.
Labelling of fibres in sections cut from four different resin blocks (six fibres/block) using the same preparation of CBM-gold complex, (a, b) unbleached fibres and (c, d) bleached fibres. The same alphabet shown for each replicate depicts no significant difference.

labelled unbleached and fully bleached fibres, where the decrement of CBM-gold particles after bleaching is obvious (Figure 4b).

Reproducibility of *Ct*CBM6-gold counts and distribution

The optimised CBM-gold method was replicated for unbleached and fully bleached pulp fibres taken from four different resin blocks. A difference in total gold counts obtained for individual fibres was expected because of the natural variation between trees and fibres (Donaldson et al. 2004) (Figure 5). The combined data for fibre labelling from each resin block for both unbleached (Figure 5c) and fully bleached fibres (Figure 5d) showed no significant differences and the variations are supposed to be within the natural differences between populations of the fibres analysed.

The distribution patterns of xylan are very similar for the different fibre batches from each resin block for unbleached fibres (Figure 6a) and fully bleached fibres (Figure 6b) concerning the cross sections of the secondary cell wall layers. Unbleached fibres show no difference in the layers S1, S2 and S3 (Figure 6a). The xylan distributions of fully bleached fibres indicate that the S1 and S3 cell wall layers contain more xylan than the S2 layer for all replicates (Figure 6b). Bleaching removes a significant amount of xylan from all three cell wall layers but the xylan removal in the S2 layer is the most significant (Figure 6b). The conclusion is that the labelling results concerning xylan removal during bleaching are plausible and reliable.

Conclusions

A reproducible *Ct*CBM6-gold label colloid technique was developed to map xylan distribution across the secondary cell wall layers of pulp fibre walls. The size of the gold colloid marker appears to be an important factor when preparing a CBM-gold colloid conjugate. The preparation of a stock solution as well as the applied buffer for diluting the conjugate affected the affinity of the probe to xylan. The counts of gold particles across the different secondary cell wall layers reflect the xylan distribution, which was changed during the bleaching process. The *Ct*CBM6-gold label tool contributes to understanding the complexity

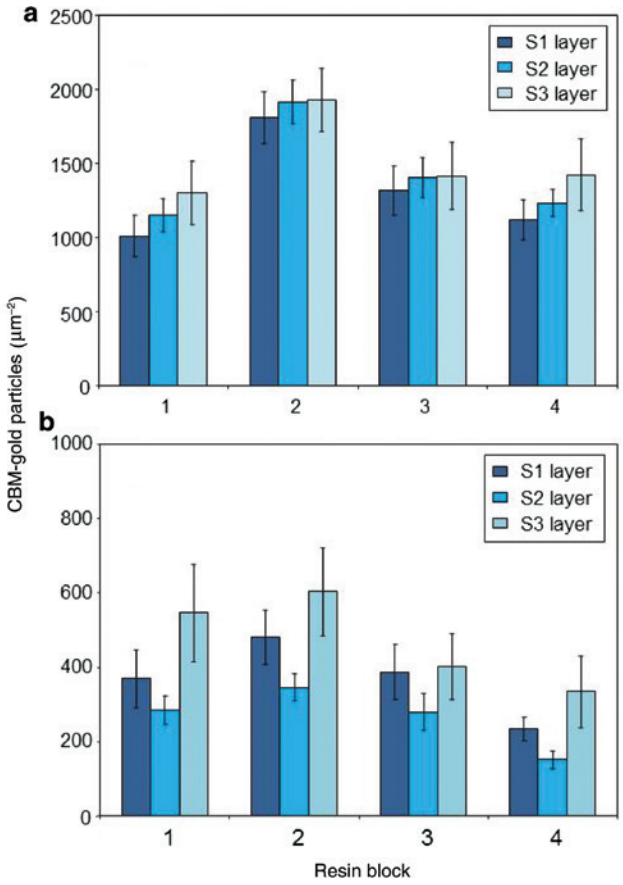

Figure 6: Reproducibility of xylan distribution patterns shown for four replicate experiments.
Distribution of xylan obtained across the secondary wall layers (a) unbleached fibres and (b) bleached fibres. Error bars indicate standard error; $n = 6$.

of the hardwood fibre cell wall and its behaviour during bleaching. It is not only useful for basic research but also as a monitoring tool of technological processes.

Acknowledgements: The authors acknowledge and are thankful to the technical staff at the Biorefinery Industry development Facility for assisting with the HPLC analysis, the University of KwaZulu-Natal Microscopy and Microanalysis unit for use of their equipment, and the Council of Scientific and Industrial Research for funding.

References

Altaner, C., Hapca, A.I., Knox, J.P., Jarvis, M.C. (2007) Detection of β-1-4-galactan in compression wood of Sitka spruce [*Picea sitchensis* (Bong.) Carrière] by immunofluorescence. Holzforschung 61:311–316.

Blumentritt, M., Gardner, D.J., Cole, B., J.W., Shaler, S.M. (2016) Influence of hot-water extraction on ultrastructure and distribution of glucomannans and xylans in poplar xylem as detected by gold immunolabeling. Holzforschung 70: 243–252.

Boraston, A., Mclean, B., Kormos, J., Alam, M., Gilkes, N., Haynes, C., Tomme, P., Kilburn, D., Warren, R. (1999) Carbohydrate-binding modules: diversity of structure and function. R. Soc. Ch. 246:202–211.

Chunilall, V., Bush, T., Larsson, P. T., Iversen, T., Kindness, A. (2010) A CP/MAS 13C-NMR study of cellulose fibril aggregation in eucalyptus dissolving pulps during drying and the correlation between aggregate dimensions and chemical reactivity. Holzforschung 64:693–698.

Czjzek, M., Bolam, D.N., Mosbah, A., Allouch, J., Fontes, C.M., Ferreira, L.M., Bornet, O., Zamboni, V., Darbon, H., Smith, N.L. (2001) The location of the ligand-binding site of carbohydrate-binding modules that have evolved from a common sequence is not conserved. J. Biol. Chem. 276:48580–48587.

Daniel, G., Filonova, L., Kallas, Å.M., Teeri, T.T. (2006) Morphological and chemical characterisation of the G-layer in tension wood fibres of *Populus tremula* and *Betula verrucosa*: labelling with cellulose-binding module CBM1 Hj Cel7A and fluorescence and FE-SEM microscopy. Holzforschung 60:618–624.

Ding, S., Xu, Q., Ali, M.K., Baker, J.O., Bayer, E.A., Barak, Y., Lamed, R., Sugiyama, J., Rumbles, G., Himmel, M.E. (2006) Versatile derivatives of carbohydrate-binding modules for imaging of complex carbohydrates approaching the molecular level of resolution. Biotechniques 41:435.

Donaldson, L.A., Grace, J., Downes, G.M. (2004) Within-tree variation in anatomical properties of compression wood in radiata pine. IAWA J. 25:253–271.

Dykstra, M.J., Reuss, L.E. (2003) Specimen preparation for electron microscopy. In: Biological Electron Microscopy. Springer, International Publishing AG. pp. 1–498.

Fernando, D., Daniel, G. (2008) Exploring Scots pine fibre development mechanisms during TMP processing: Impact of cell wall ultrastructure (morphological and topochemical) on negative behaviour. Holzforschung 62:597–607.

Filonova, L., Kallas, Å.M., Greffe, L., Johansson, G., Teeri, T.T., Daniel, G. (2007a) Analysis of the surfaces of wood tissues and pulp fibers using carbohydrate-binding modules specific for crystalline cellulose and mannan. Biomacromolecules 8:91–97.

Filonova, L., Gunnarsson, L.C., Daniel, G., Ohlin, M. (2007b) Synthetic xylan-binding modules for mapping of pulp fibres and wood sections. BMC Plant Biol. 7:54–64.

Gao, J., Kim, J.S., Terziev, N., Allegretti, O., Daniel, G. (2014) Chemical and ultrastructural changes in compound middle lamella (CML) regions of softwoods thermally modified by the Termovuoto process. Holzforschung 68:849–859.

Goodman, S., Hodges, G., Trejdosiewicz, L., Livingston, D. (1981) Colloidal gold markers and probes for routine application in microscopy. J. Microsc. 123:201–213.

Hashimoto, H. (2006) Recent structural studies of carbohydrate-binding modules. Cell. Mol. Life Sci. 63:2954–2967.

Hausalo, T. (1995) Analysis of wood and pulp carbohydrates by anion exchange chromatography with pulsed amperometric detection. 8th International Symposium on Wood and Pulping Chemistry, Helsinki, Finland: 131–136.

Hildén, L., Daniel, G., Johansson, G. (2003) Use of a fluorescence labelled, carbohydrate-binding module from *Phanerochaete chrysosporium* Cel7D for studying wood cell wall ultrastructure. Biotechnol. Lett. 25:553–558.

Horisberger, M. (1979) Evaluation of colloidal gold as a cytochemical marker for transmission and scanning electron-microscopy. Biol. Cellulaire 36:253–258.

Horisberger, M., Vauthey, M. (1984) Labelling of colloidal gold with protein. Histochemistry 80:13–18.

Kim, J.S., Gao, J., Terziev, N., Allegretti, O., Daniel, G. (2015) Chemical and ultrastructural changes of ash wood thermally modified (TMW) using the thermo-vacuum process: II. Immunocytochemical study of the distribution of noncellulosic polysaccharides. Holzforschung 69:615–625.

McCartney, L., Blake, A.W., Flint, J., Bolam, D.N., Boraston, A.B., Gilbert, H.J., Knox, J.P. (2006) Differential recognition of plant cell walls by microbial xylan-specific carbohydrate-binding modules. Proc. Natl. Acad. Sci. U.S.A. 103:4765–4770.

Mclean, B.W., Boraston, A.B., Brouwer, D., Sanaie, N., Fyfe, C.A., Warren, R.A., Kilburn, D.G., Haynes, C.A. (2002) Carbohydrate-binding modules recognize fine substructures of cellulose. J. Biol. Chem. 277:50245–50254.

Oliveira, C., Carvalho, V., Domingues, L., Gama, F.M. (2015) Recombinant CBM-fusion technology – applications overview. Biotechnol. Adv. 33:358–369.

Pattathil, S., Avci, U., Zhang, T., Cardenas, C.L., Hahn, M.G. (2015) Immunological approaches to biomass characterization and utilization. Front Bioeng. Biotechnol. 3:173.

Polak, J., Van Noorden, S. (1987) An introduction to immunocytochemistry: current techniques and problems. In: Microscopy Handbook 11. Oxford University Press, Oxford.

Rocklin, R.D., Pohl, C.A. (1983) Determination of carbohydrates by anion exchange chromatography with pulsed amperometric detection. J. Liq. Chromatogr. 6:1577–1590.

Shoseyov, O., Shani, Z., Levy, I. (2006) Carbohydrate binding modules: biochemical properties and novel applications. Microbiol. Mol. Biol. R. 70:283–295.

Sixta, H. (2006) Pulp properties and applications. In: Handbook of Pulp. Wiley-VCH Verlag GmbH, Weinheim, Germany. pp. 1009–1067.

Slot, J.W., Geuze, H.J. (1981) Sizing of protein A-colloidal gold probes for immunoelectron microscopy. J. Cell Biol. 90:533–536.

Slot, J.W., Geuze, H.J. (1985) A new method of preparing gold probes for multiple-labeling cytochemistry. Eur. J. Cell Biol. 38:87–93.

Stannard, L.M. (1998) Direct immunogold labeling of herpesvirus suspensions. Methods Mol. Med. 10:83–173.

Timell, T. (1967) Recent progress in the chemistry of wood hemicelluloses. Wood Sci. Technol. 1:45–70.

Verma, A.K., Bule, P., Ribeiro, T., Brás, J.L.A., Mukherjee, J., Gupta, M.N., Fontes, C.M.G.A., Goyal, A. (2015) The family 6 Carbohydrate Binding Module (CtCBM6) of glucuronoxylanase (CtXynGH30) of *Clostridium thermocellum* binds decorated and undecorated xylans through cleft A. Arch. Biochem. Biophys. 575:8–21.

Wilson, J., Tabke, R. (1974) Influences of hemicelluloses on acetate processing in high catalyst systems. Tappi 57:77–80.

Wollboldt, R.P., Zuckerstätter, G., Weber, H.K., Larsson, P.T., Sixta, H. (2010) Accessibility, reactivity and supramolecular structure of *E. globulus* pulps with reduced xylan content. Wood Sci. Technol. 44:533–546.